

# Influence of Annealing Duration on the Structural, Optical and Electrical Properties of ZnO Layers Deposited Using the Dip-Coating Method

May Zin Toe<sup>1,a</sup>, Atsunori Matsuda<sup>2,b</sup>, Khatijah Aisha Binti Yaccob<sup>1,c</sup>  
and Swee-Yong Pung<sup>1,d\*</sup>

<sup>1</sup>School of Materials and Mineral Resources Engineering, Engineering Campus, Universiti Sains Malaysia, 14300 Nibong Tebal, Penang, Malaysia

<sup>2</sup>Department of Electrical and Electronic Information Engineering, Toyohashi University of Technology, 1-1 Hibarigaoka, Tempaku-cho, Toyohashi 441-8580, Japan

<sup>3</sup>Department of Physics, University of East Yangon, Thanlyin 11292, Yangon Division, Myanmar

<sup>a</sup>mayzintoe84@gmail.com, <sup>b</sup>matsuda@ee.tut.ac.jp, <sup>c</sup>mraisha@usm.my, <sup>d\*</sup>sypung@usm.my

**Keywords:** Dip coating, ZnO layers, annealing,

**Abstract.** Zinc sol deposited via dip coating on Fluorine-doped Tin Oxide (FTO) coated glasses were annealed at 450 °C in normal ambient to form ZnO layers. The effect of annealing durations, i.e. 30, 60, 90, and 120 min on their surface morphology, crystallinity, optical, electrical and Dye-Sensitized Solar Cells (DSSCs) performance were studied. The XRD analyses indicated the formation of wurtzite ZnO after 60 min of annealing. It is noted that the ZnO layers annealed at 60-120 min showed good crystal quality attributed to its sharp, narrow and strong diffraction peaks. Generally, ZnO layers with uniform thickness have been deposited on the FTO coated glasses. The thickness of ZnO layers decreased from 0.88, 0.78, 0.76, and 0.73 µm when the annealing duration increased from 30 to 120 min due to removal of hydrocarbons from the zinc sol. The O at. % increased with annealing duration, indicating that more oxygen reacted with zinc to form ZnO. The ZnO thin film annealed at 60 min had relatively low sheet resistance (9.6 Ω/□) with optical bandgap of 3.04 eV. This suggests that ZnO layers annealed at 60 min have the largest amount of oxygen vacancies that contributed electrons for charges transportation in the layers. Besides, the Room Temperature Photoluminescence (RTPL) analyses showed that the ZnO thin film annealed for 60 min showed  $I_{UV}/I_{Vis}$  ratio = 0.89, suggesting better crystal quality compared to shorter annealing duration.

## Introduction

Transparent conductive coatings (TCCs) based on semiconductor oxides in particular have a wide range of applications such as in optical devices, photovoltaic cells and displays. Zinc oxide (ZnO) is a semiconductor oxide nanomaterial that crystallizes in wurtzite structure and have direct bandgap of 3.37eV with an exciton binding energy of 60 meV at room temperature. Due to these unique properties, ZnO is a potential candidate for piezoelectric transducers [1], optical waveguides [2], acousto-optic media [3], conductive gas sensors [4] and TCCs[5].

Development of a cost- and time-effective deposition technique to produce ZnO layer with controlled uniform thickness and electrical property is needed for the above applications. Many deposition techniques have been established for ZnO layer deposition, for instances, sol-gel [6], hydrothermal [7], atomic layer deposition [8] and chemical vapor deposition [9]. It is noted that these deposition techniques affect the structural, optical and electrical properties of ZnO layers due to variation in compositions [10], crystalline phases [11] and microstructures [10], or inhomogeneous multilayer [12] or composite structure [13].

Dip-coating technique has been chosen in this work because of its simple and low cost process. It is suitable for mass production and easy to up-scale for deposition on larger size of substrates. Nevertheless, this process suffers from uneven thickness, which could affect the electrical conductivity of the ZnO layers. In addition, the reduction of deposition thickness after annealing is not explained in literature. A ZnO seed layer was pre-coated on the surface of FTO glass substrates in order to facilitate the deposition of ZnO layers in subsequent dip-coating process. This improved

the uniformity of ZnO thickness and achieved full deposition (coverage) of ZnO layer on the FTO glass substrates. The purposes of this work are to study the effects of annealing duration on the structural, optical and electrical properties of ZnO layers. The mechanism of reduction of ZnO layers' thickness after annealing also discussed based on the findings in this work.

### Experimental Setup

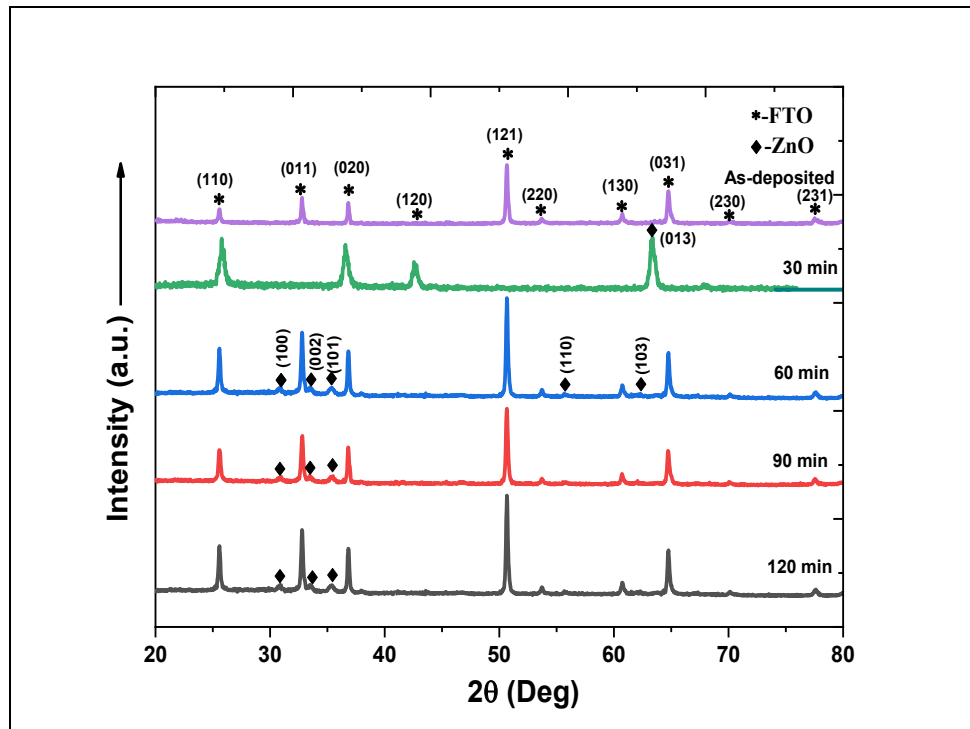
The pre-cut FTO coated glasses ( $2 \times 3 \text{ cm}^2$ , sheet resistance of  $10\text{--}15 \Omega \text{ sq}^{-1}$ ) were ultrasonically cleaned using detergent (Decon 90, UK) for 15 min and then rinsed with 2-propanol, ethanol and DI water. The substrates were dried in oven for 1 hr at  $100^\circ\text{C}$ . Next, zinc sol was deposited on the glass substrates by dip-coating. This was done by dipping vertically the glass substrates into the precursor solution. The solution was a mixture of 0.125 M zinc acetate dihydrate and 0.125 M diethanolamine. The dipping process was carried out using a dip-coating controller (Aiden). The dipping parameters were kept consistent, i.e. down-speed was maintained at 5.0 mm/s with a dwell time of 10 s and a withdrawing speed of 0.1 mm/s. Subsequently, the substrates were dried at  $100^\circ\text{C}$  for 15 min in an oven. The dip-coating was repeated 3 cycles to achieve complete coverage and uniform thickness of zinc sol on the glass substrates. The substrates were annealed in normal ambient at  $450^\circ\text{C}$  for 30, 60, 90 and 120 min.

The crystal phase of ZnO layers characterized by X-ray diffractometry (XRD, Rigaku RINT 2500) with a  $\text{Cu K}\alpha$  radiation ( $\lambda = 1.54059 \text{ \AA}$ ). The microstructures of ZnO layers were observed by field emission scanning electron microscope (FE-SEM, HITACHI, S-4800) using accelerating voltage of 40 kV. The average film thickness was measured using Image J software. The optical properties of ZnO layers were analysed using an ultraviolet-visible near infrared spectrophotometer (V-670, JASCO Corporation, scanning range: 350–700 nm), a Raman spectroscopy (NRS-3100, JASCO Corporation) and room temperature photoluminescence (RTPL) spectroscopy (KIMMON KOHA, excitation wavelength: 325 nm).

### Results and Discussion

#### Structural properties of ZnO layers

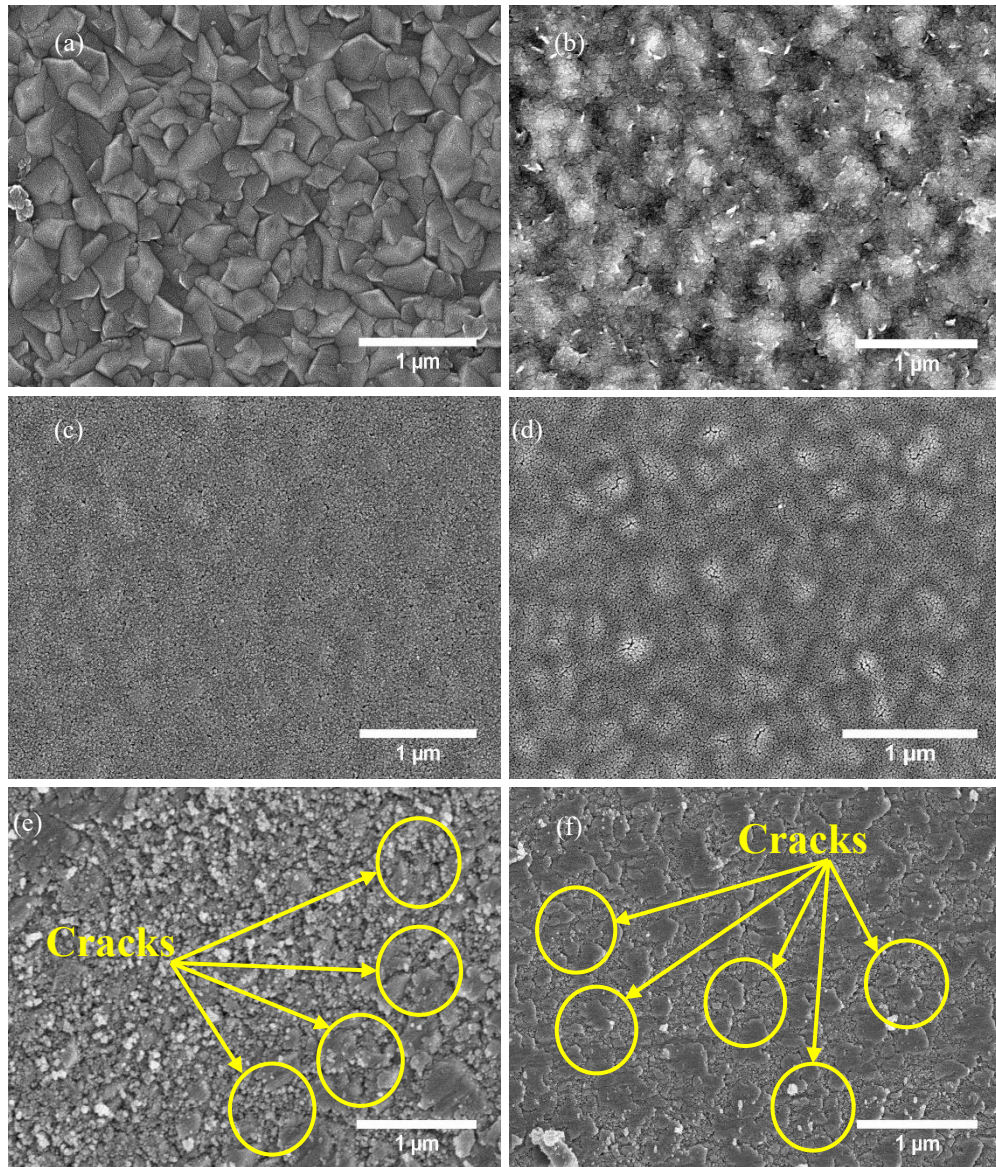
The ZnO layers was annealed at  $450^\circ\text{C}$  but with different durations, i.e. varied from 0 (as-deposited), 30, 60, 90 and 120 min. Fig 1 shows the XRD pattern of ZnO layers annealed at different durations. The Bragg diffractions at  $26.49^\circ$ ,  $33.62^\circ$ ,  $37.68^\circ$ ,  $51.49^\circ$ ,  $54.46^\circ$ ,  $61.49^\circ$ ,  $64.15^\circ$ ,  $65.51^\circ$ ,  $70.77^\circ$  and  $78.07^\circ$  correspond to (110), (011), (020), (121), (220), (130), (112), (031), (230) and (231) of tin oxide with crystal structure of FTO JCPDS (98-006-3707). No diffraction peaks related to ZnO were measured for as-deposited thin film and thin forms annealed for 30 min. Nevertheless, diffraction peaks associated with ZnO were found at a longer annealing duration, i.e. 60 – 120 min. The diffraction peaks at  $31.72^\circ$ ,  $34.37^\circ$ ,  $36.22^\circ$ ,  $56.29^\circ$  and  $62.38^\circ$  correspond to (100), (002), (101), (110) and (103) planes of hexagonal wurtzite ZnO (JCPDS-96-100-0063) with lattice constants of  $a=b=3.24 \text{ \AA}$  and  $c=5.20 \text{ \AA}$ .



**Fig. 1.** XRD pattern of ZnO layers annealed at 450°C for different durations.

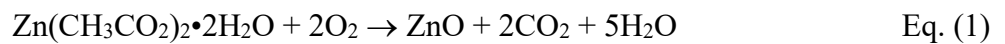
### Morphological properties of ZnO layers

Fig. 2 (a) shows the morphology of bare FTO. The FTO thin film composed of large grains ( $0.32 \pm 0.02$  nm,  $n=30$ ) with uneven surface. The large grains of FTO could be still observed when a layer of zinc sol was coated on the surface of FTO glass substrate in Fig. 2 (b). The thin film layers annealed at 30 and 60 min show homogeneous closely packed and tiny particles ( $< 50$  nm) in Fig. 2 (c) and (d). No pinhole and crack could be found on the surface of layers. A longer annealing duration, i.e. 90 and 120 min, producing larger particles as seen in Fig. 2 (e) and (f). This is an indication of Ostwald ripening effect, where tiny particles dissolved and re-deposited to form large particles [14]. Nevertheless, these layers have porous structure with loosely bound particles on the substrate surface. In addition, cracks were found on these layers as highlighted in Fig. 2 (e) and (f).



**Fig. 2.** FESEM images of (a) bare FTO, and ZnO layers annealed at 450°C for (b) 0 (as-deposited), (c) 30, (d) 60, (e) 90 and (f) 120min

Fig 3 (a)-(e) shows the cross-sectional view of ZnO layers thickness annealed at different durations. The thickness of as-deposited zinc acetate thin film is 0.89  $\mu\text{m}$ . By extending the annealing duration, the thickness of layers decreased from 0.88, 0.78, 0.76 and 0.73  $\mu\text{m}$  for 30, 60, 90 and 120 min., respectively as plotted in Fig 3 (f). The reduction of thickness was due to oxidation of zinc acetate into ZnO and burning off of hydrocarbons from the ZnO layers as described in Eq. (1), releasing by products such water and carbon dioxide. A longer annealing time allowed more complete oxidation of zinc acetate. Long annealing duration, i.e. 90 and 120 min, were not favoured as cracks, loosely bound particles and porous structures were observed on the surface of ZnO layers.





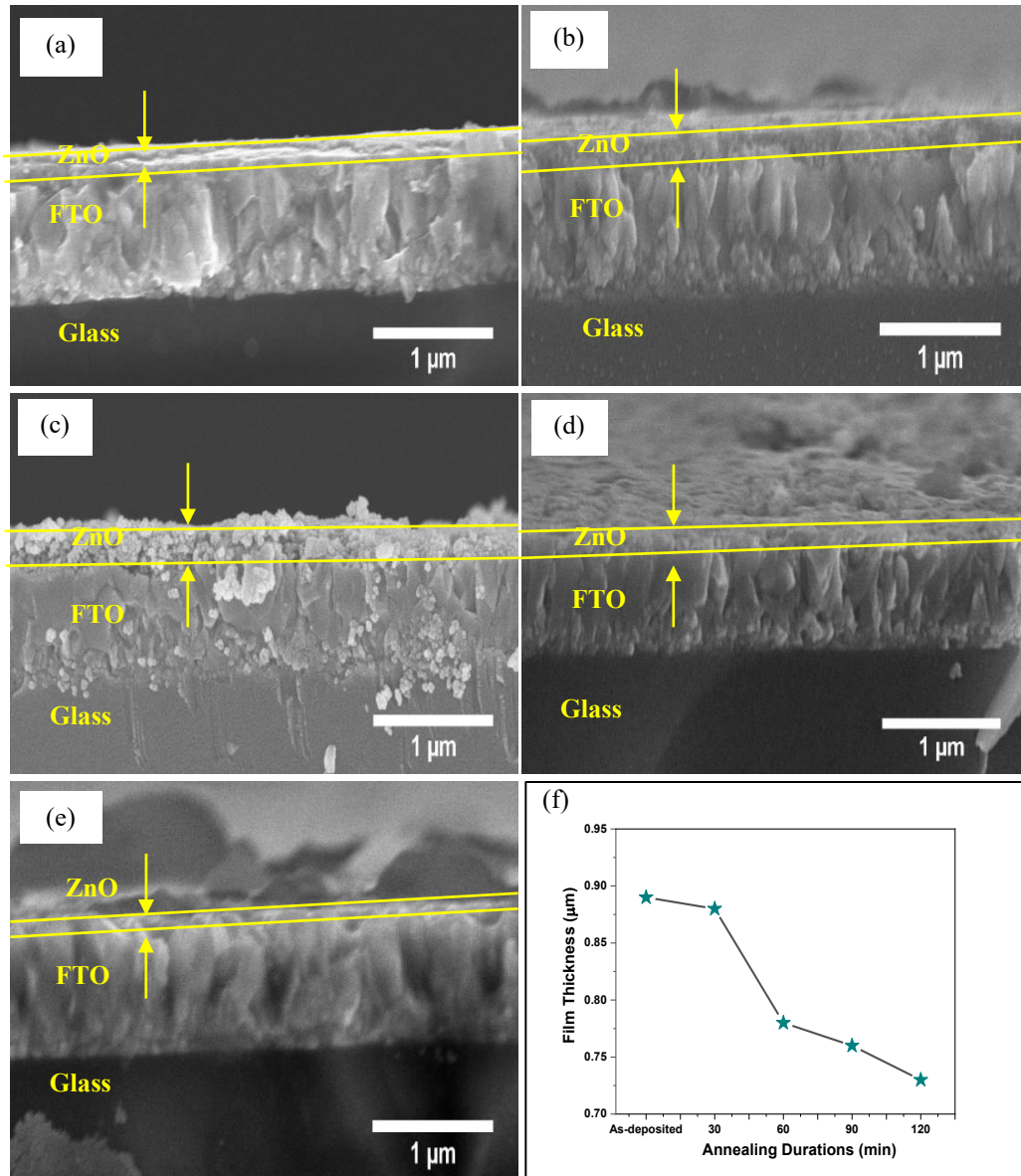


**Fig. 3.** FESEM cross-sectional images of ZnO layers at annealing temperature 450°C for (a) 0 (as-deposited), (b) 30, (c) 60, (d) 90, (e) 120 min and (f) thin film thickness versus annealing durations.

EDX measurement was performed to determine the atomic ratio of Zn to O. The atomic ratio of Zn and O is shown in Fig 4. The O at. % increased with annealing duration, indicating that more oxygen reacted with zinc to form ZnO. Nevertheless, this could affect the sheet resistance of ZnO layers as it is known that electrons are usually contributed from oxygen vacancies [15, 16]. The result shows that ZnO thin film annealed at 60 min has higher Zn atoms as compared to O atoms, indicating that it has the largest oxygen vacancies in the film. The presence of ZnO was not detected by XRD in Fig. 1 for as-deposited film and film annealed for 30 min. Thus, ZnO formed after annealing of more than 60 min.

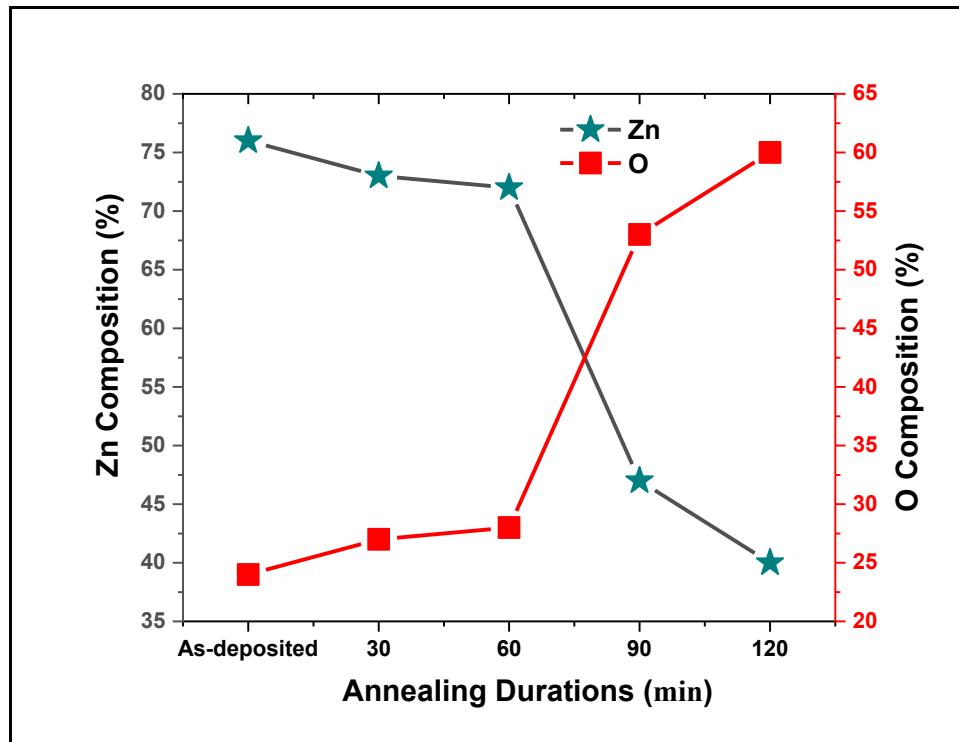
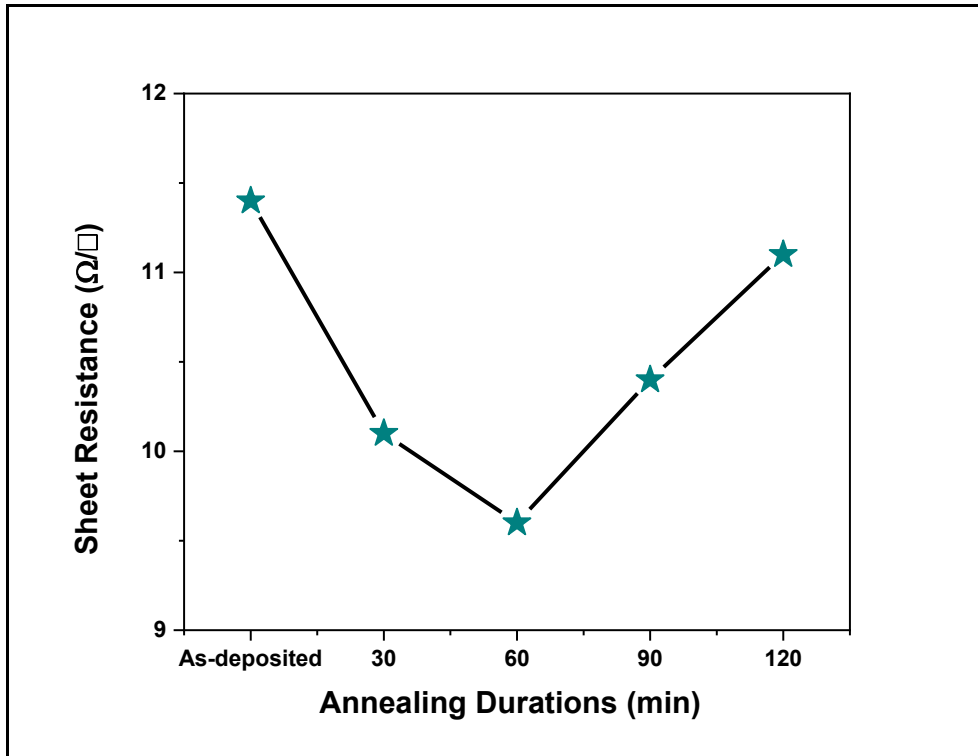


Fig. 4. EDX analysis of ZnO layers annealed at 450 °C for different durations.

### Optical properties of ZnO layers

The effect of annealing duration on the sheet resistance of ZnO layers is displayed in Fig. 5. The as-deposited thin film (zinc acetate) recorded sheet resistance of  $11.4 \Omega/\square$ . The sheet resistance decreased with increasing annealing duration, achieving  $9.6 \Omega/\square$  at 60 min. Formation of ZnO layers which contained many oxygen vacancies was believed the cause of this observation. It is known that charge carriers transportation in ZnO layers is via electrons (n-type, majority charge carriers). These electrons were mainly contributed from the oxygen vacancies in ZnO layers [17].

Nevertheless, the sheet resistances of ZnO layers increased with pro-long annealing duration. It was measured  $11.1 \Omega/\square$  after annealed for 120 min. The increase of O at. % in Fig. 4 (EDX) with pro-long annealing indirectly indicates the reduction of oxygen vacancies in ZnO layers. Since oxygen vacancies were the main source of electrons for charges transportation, the reduction of oxygen vacancies in ZnO layers would increase the sheet resistance after pro-long annealing. In addition, the presence of cracks, loosely bounded particles and porous structure in ZnO layers (Fig 2. (e) and (f)) could also increase the resistance for the movement of charge carriers in the ZnO layers.



**Fig. 5.** Sheet resistance of ZnO layers annealed at 450 °C for different durations.

Fig. 6 (a) shows the optical transmission spectra of ZnO layers recorded in the wavelength region of 350–800 nm for different annealing durations. In general, the ZnO layers are highly transparent with an average transmission of  $75.0 \pm 2.8$  % in the visible range. Fig. 6 (b) shows the absorption of layers. The layers have absorption edges at  $\sim 376$  nm which correspond to optical bandgap of ZnO. Fig. 6 (c) shows the Tauc plot of layers annealed at different duration. It was found that the optical bandgap increased with annealing duration, i.e. from 2.71 (as-deposited) to 3.13 eV (120 min) as shown in Fig. 6 (d). The optical bandgap was closed to the literature report value, i.e. 3.37 eV [18]. Pro-long annealing duration allowed more oxygen to react with zinc in order to form ZnO.

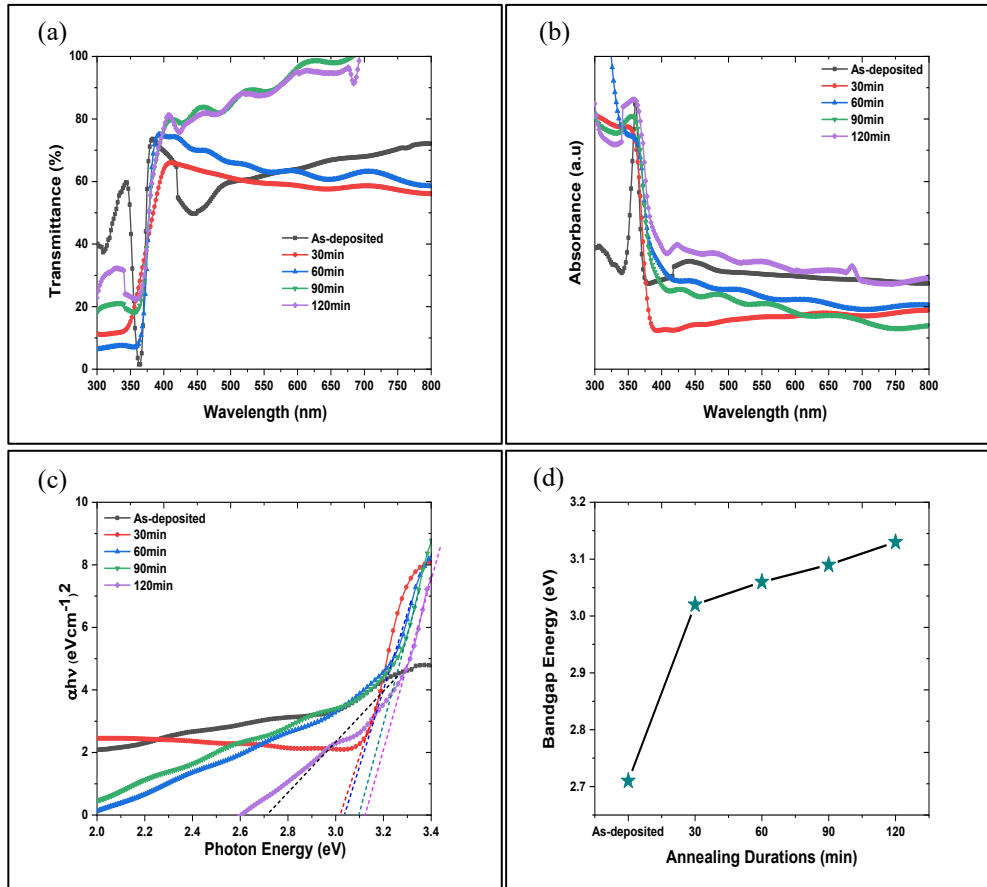


**Fig. 6.** (a) Transmittance, (b) absorbance, (c) Tauc plot and (d) optical bandgap of ZnO layers annealed at 450 °C for different durations

Fig. 7 shows the Raman spectra of layers annealed at different durations. The Raman shifts at 458 and 564  $\text{cm}^{-1}$  associated with  $E_2$  (High) and  $A_1$  (LO) modes are observed. The  $E_2$  (High) mode is related to vibration of oxygen atoms in ZnO. Thus, presence of  $E_2$  (High) was an indication of ZnO formation. The presence of  $A_1$  (LO) indicates that the layers contained crystal defects such as oxygen vacancies [19]. This observation is agreed well with the finding in the EDX analysis that the layers were lacked of oxygen (Fig. 4).



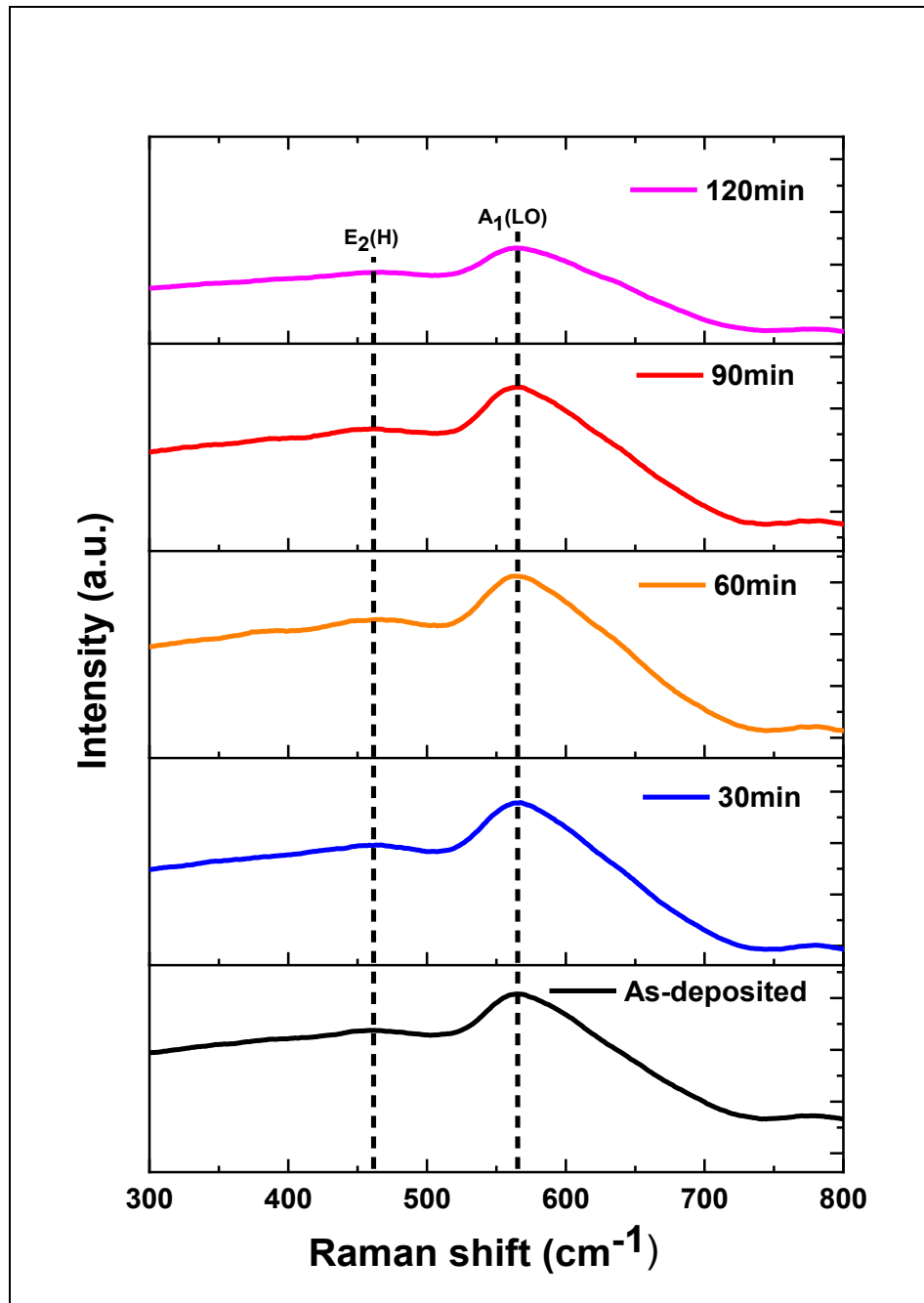


**Fig. 7.** Raman spectra of ZnO layers annealed at 450 °C for different durations

The room temperature PL spectrum of ZnO layers with various annealing durations is shown in Fig 8. A sharp UV emission (NBE) (385 nm) accompanied with a broad visible light emission (defect related) in green-orange band (480–750 nm) are observed in all layers as displayed in Fig 8 (a). The effect of annealing temperature on the maximum peaks of UV and visible light emission were negligible as it was random as shown in Fig 8 (b) and (c). Nevertheless, the  $I_{UV}/I_{vis}$  ratio increased with increasing duration as shown in Fig 8 (d), although a slight drop was observed at 120 min. The result suggests that less crystal defects present in ZnO layers at pro-long annealing duration. The crystal quality of layers was improved as more oxygen were allowed to react with zinc acetate for the formation of ZnO.

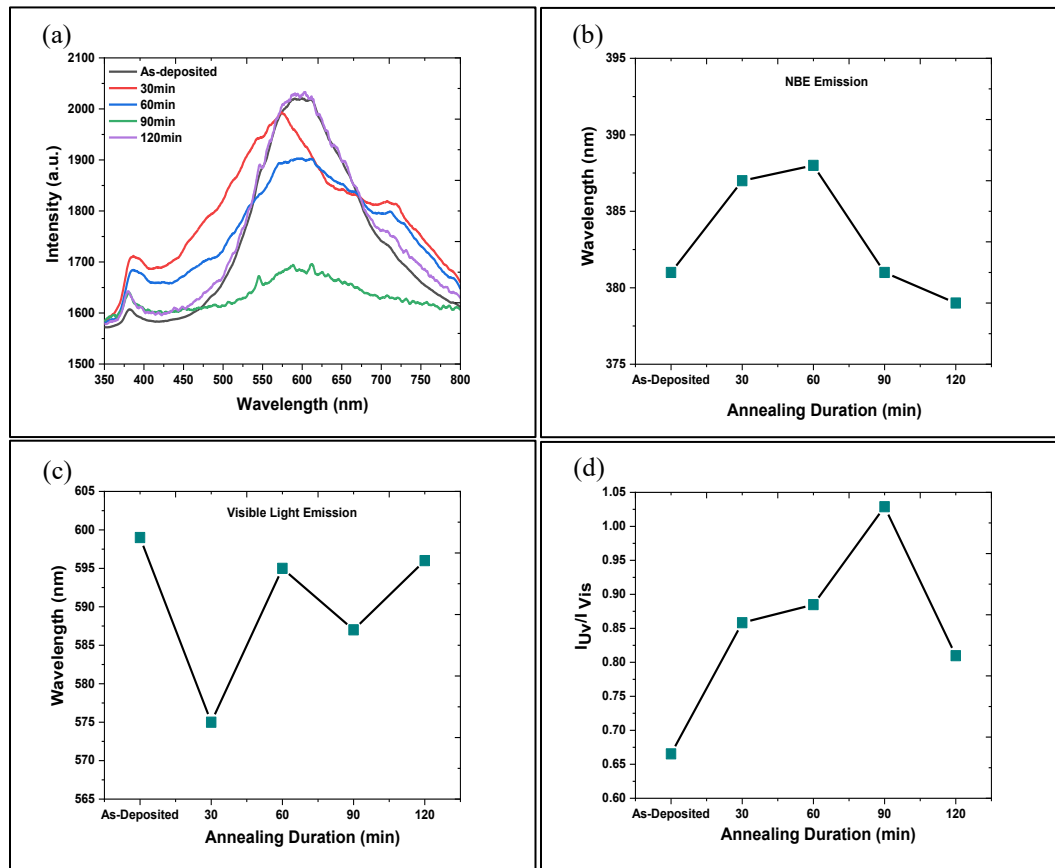


**Fig. 8.** (a) Room temperature photoluminescence, (b) shift of maximum peak in UV regime (NBE), (c) shift of maximum peak in visible light regime (defect-related emission), (d)  $I_{UV}/I_{VIS}$  ratio of ZnO layers annealed at different durations

Table 1 summarizes the findings of ZnO layers annealed at 450°C with different durations. This table shows that the length of annealed duration time affected the crystal growth. A longer annealing time provided more reaction time and thermal energy that were required for crystal growth and recrystallization. After maintaining the annealing duration over 30 min, dense and hexagonal crystal grains were obtained. The appropriate annealing duration to produce ZnO thin film was 60 min. At this annealing duration, no glass deformation and thin film delamination were observed. Besides, the analyses indicate that the thin film was ZnO with good thickness uniformity and crystal quality ( $I_{UV}/I_{VIS}$  ratio = 0.89). The ZnO thin film had relatively low sheet resistance ( $9.8 \Omega/\square$ ) with optical bandgap of 3.04 eV.

**Table 1.** Structural and optical properties of ZnO layers annealed at different annealing durations

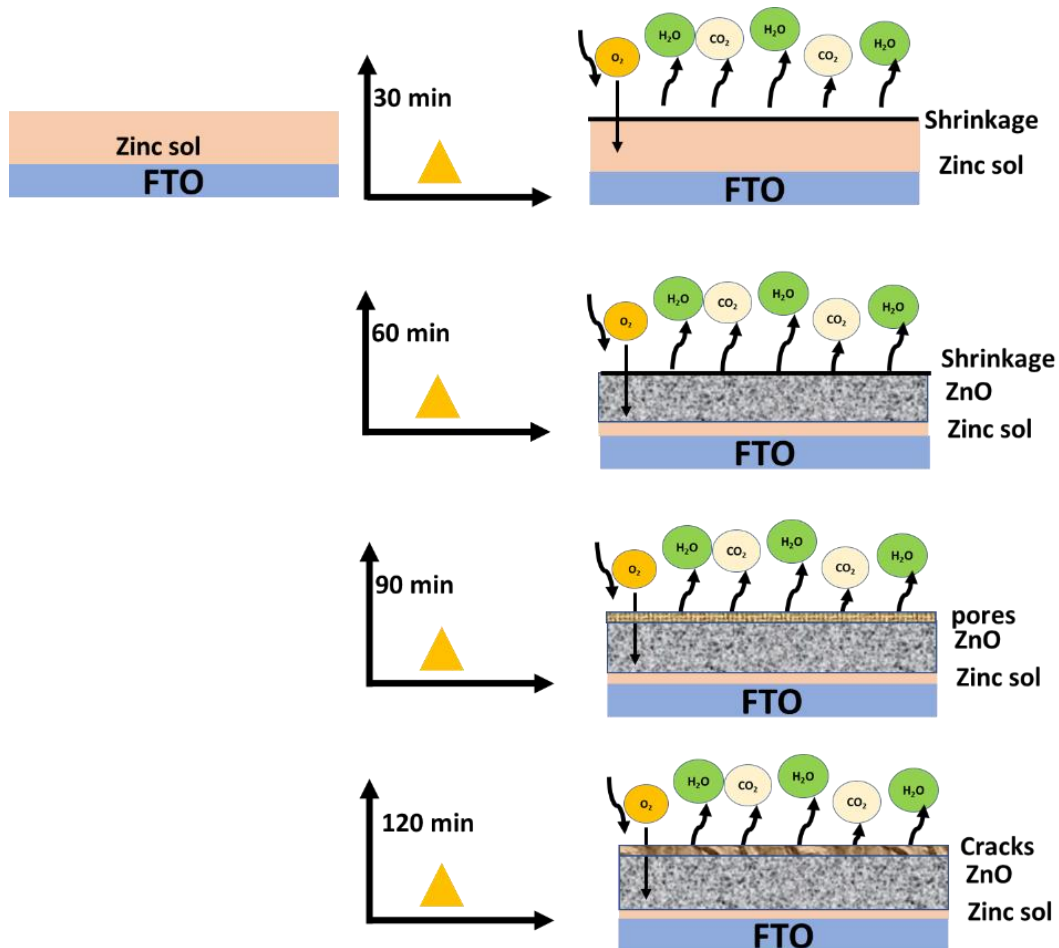
N o.	Observation	As-deposited	30 min	60 min	90 min	120 min
1	Substrate deformation	No	No	No	Yes	Yes
2	Detection of ZnO (XRD)	No	No	Yes	Yes	Yes
3	Thickness uniformity (FESEM)	Yes	Yes	Yes	Yes	Yes
4	Thin film delamination (FESEM)	No	No	No	No	No
5	Zn : O atomic ratio (EDX)	76:24	73:27	69:31	53:47	24:76
6	Sheet resistance ( $\Omega/\square$ )	11.4	10.1	9.6	10.4	11.1
7	Optical bandgap (eV) (UV-Vis)	2.71	3.02	3.06	3.09	3.13
8	Raman shift: $E_2$ (High) mode	No	No	Yes	Yes	Yes
9	Crystal quality (RTPL: $I_{UV}/I_{VIS}$ ratio)	0.67	0.86	0.89	1.03	0.81

Fig. 9 illustrates the annealing effect on the structural, optical and electrical properties of ZnO layers based on the observation from FESEM images, XRD analyses and sheet resistance

measurement. In short annealing duration (30 min), water vaporization and oxidation of hydrocarbons happened on the surface of thin film. Only a small portion of zinc sol near the sub-surface could be decomposed and oxidized into ZnO. The presence of this ZnO was too little to be detected by XRD and Raman spectroscopy. Most of the deposited thin film still remained as zinc sol. As a result, the thin film had the highest sheet resistance ( $11.4 \Omega/\square$ ), narrow bandgap (2.71 eV) and poor  $I_{UV}/I_{vis}$  ratio (0.67) in RTPL measurement.

By prolonging the annealing duration to 60 min, more water and hydrocarbons were removed from thin film. More zinc sol was oxidized into ZnO as signals associated with ZnO were detected by both XRD and Raman spectroscopy. This caused shrinkage of thin film thickness from  $0.89 \mu\text{m}$  to  $0.78 \mu\text{m}$ . The thin film had the lowest sheet resistance ( $9.6 \Omega/\square$ ), wide bandgap (3.06 eV) and better  $I_{UV}/I_{vis}$  ratio (0.89). Nevertheless, it is believed that there were still some zinc sol remained particularly at the parts that close to FTO substrate. The oxygen from ambient needed more time to diffuse into the layers and to oxidize the zinc sol.

Further annealed the thin film to 120 min resulted in the formation of pores, cracks, shrinkage and delamination of thin film due to fully decomposition and oxidation of zinc sol into ZnO. The presence of these crystal defects in the thin film increased the sheet resistance to  $11.1 \Omega/\square$ .



**Fig. 9.** Effect of annealing duration on the structural of ZnO layers that annealed at 450 °C.

## Conclusions

ZnO layers were deposited on FTO glass substrates using dip coating method. Process optimization was performed by varying annealing durations (As-deposited, 30, 60, 90 and 120 min) at the annealing temperature 450°C. The annealing duration determined the crystal growth and completeness of oxidation of zinc sol to form ZnO. Short annealing duration (< 30 min) was insufficient to oxidize the zinc sol into ZnO. ZnO was detected by XRD analysis when the layers

were annealed more than 60 min. Nevertheless, long annealing duration (120 min) caused thin film peeling or cracks and even significant deformation on glass substrates. The study showed that ZnO thin film annealed at 60 min has the lowest sheet resistance ( $9.6 \Omega/\square$ ) with optical bandgap of 3.04 eV and good  $I_{UV}/I_{Vis}$  ratio = 0.89.

### Acknowledgement

The authors gratefully acknowledge the financial support of Ministry of Higher Education, Malaysia for providing the research funding under Fundamental Research Grant Scheme (FRGS) (FRGS/1/2020/TK0/USM/02/27) to conduct this project and the support from the USM Fellowship.

### Research Data Policy and Data Availability Statements

The datasets generated during and/or analysed during the current study are available from the corresponding author on reasonable request.

### References

- [1] P.-C. Lee, Y.-L. Hsiao, J. Dutta, R.-C. Wang, S.-W. Tseng, C.-P. Liu, "Development of porous zno thin films for enhancing piezoelectric nanogenerators and force sensors", *NANO ENERGY*, 82 (2021)105702.
- [2] L. Agarwal, R. Singh, S. Tripathi, "Structural and optical characterization of ezo thin film for application in optical waveguide," *Advances in vlsi, communication, and signal processing*, D. Harvey, 683, Singapore, (2021)109-115.
- [3] M. Hanif, V. Jeoti, M. R. Ahmad, M. Z. Aslam, S. Qureshi, G. Stojanovic, "Fem analysis of various multilayer structures for cmos compatible wearable acousto-optic devices", *Sensors*, 21 (2021)7863.
- [4] A. I. Khudiar, A. M. Ofui, "Effect of pulsed laser deposition on the physical properties of zno nanocrystalline gas sensors", *Opt.Mater.*, 115 (2021)111010.
- [5] M. Z. Toe, S.-Y. Pung, K. A. B. Yaacob, S. S. Han, "Effect of dip-coating cycles on the structural and performance of zno thin film-based dssc", *Arab.J.Sci.Eng*, 46 (2021)6741-6751.
- [6] J. Soli, S. Kachbouri, E. Elaloui, C. Charnay, "Role of surfactant type on morphological, textural, optical, and photocatalytic properties of zno nanoparticles obtained by modified sol-gel", *J.Sol.Gel.Sci Technol*, 100 (2021)271-285.
- [7] G. Ahmadpour, M. R. Nilforoushan, B. S. Boroujeny, M. Tayebi, S. M. Jesmani, "Effect of substrate surface treatment on the hydrothermal synthesis of zinc oxide nanostructures", *Ceramics International*, 48 (2022)2323-2329.
- [8] K. Takase, K. Tateno, S. Sasaki, "Electrical tuning of the spin-orbit interaction in nanowire by transparent zno gate grown by atomic layer deposition", *Appl.Phys.Lett*, 119 (2021)013102.
- [9] S. Sánchez-Martín, S. Olaizola, E. Castaño, E. Urionabarrenetxea, G. Mandayo, I. Ayerdi, "Study of deposition parameters and growth kinetics of zno deposited by aerosol assisted chemical vapor deposition", *Rsc Advances*, 11 (2021)18493-18499.
- [10] N. Erdogan, T. Kutlu, N. Sedefoglu, H. Kavak, "Effect of na doping on microstructures, optical and electrical properties of zno thin films grown by sol-gel method", *J. Alloys Compd*, 881 (2021)160554.
- [11] E. Bayan, V. Petrov, M. Volkova, V. Y. Storozhenko, A. Chernyshev, "Sno<sub>2</sub>-zno nanocomposite thin films: The influence of structure, composition and crystallinity on optical and electrophysical properties", *J.Adv.Dielectr*, 11 (2021)2160008.

- 
- [12] R. Kumar, A. Dixit, "All oxide sol-gel assisted  $\text{SiO}_2/(\text{ZnO}/\text{Sn-In}_2\text{O}_3)$  n/ss dielectric/conducting multilayer based spectrally selective coating on stainless steel tubes for potential solar thermal application", *Sol. Energy*, 236 (2022)561-568.
- [13] X. Xu, S. Wang, W. Liu, Y. Chen, S. Ma, P. Yun, "An excellent triethylamine (TEA) sensor based on unique hierarchical  $\text{MoS}_2/\text{ZnO}$  composites composed of porous microspheres and nanosheets", *Sens. Actuators. B: Chem.*, 333 (2021)129616.
- [14] K. Loza, M. Epple, M. Maskos, "Stability of nanoparticle dispersions and particle agglomeration," *Biological responses to nanoscale particles* Springer, (2019)85-100.
- [15] H. S. Kang, J. S. Kang, J. W. Kim, S. Y. Lee, "Annealing effect on the property of ultraviolet and green emissions of ZnO thin films", *J. Appl. Phys.*, 95 (2004)1246-1250.
- [16] H. Liu, F. Zeng, Y. Lin, G. Wang, F. Pan, "Correlation of oxygen vacancy variations to band gap changes in epitaxial ZnO thin films", *Appl. Phys. Lett.*, 102 (2013)181908.
- [17] G. Gordillo, J. Olarte, C. Calderon, "Influence of the oxygen partial pressure on the opto-electrical properties of ZnO thin films deposited by reactive evaporation", *Physical Status Solidi B*, 220 (2000)293-297.
- [18] S. T. Tan, B. Chen, X. Sun, W. Fan, H. S. Kwok, X. Zhang, S. Chua, "Blueshift of optical band gap in ZnO thin films grown by metal-organic chemical-vapor deposition", *J. Appl. Phys.*, 98 (2005)013505.
- [19] S. S. Gaikwad, A. C. Gandhi, S. D. Pandit, J. Pant, T.-S. Chan, C.-L. Cheng, Y.-R. Ma, S. Y. Wu, "Oxygen induced strained ZnO nanoparticles: An investigation of Raman scattering and visible photoluminescence", *J. Mater. Chem. C*, 2 (2014)7264-7274.